Ground-based multispectral high-speed imaging of flickering aurora

Ryuho Kataoka,[1] Yoshizumi Miyoshi,[2] Takeshi Sakanoi,[3] Ayumi Yaegashi,[3] Yusuke Ebihara,[4] and Kazuo Shiokawa[2]

[1] It has been suggested that dispersive Alfven waves (DAWs) are capable of accelerating electrons via Landau resonance, and the interference of DAWs plays an essential role to create flickering auroral patterns. Here we show evidence that the leading front of a typical interference pattern is more energetic than the trailing part, based on ground-based high-speed imaging observations at wavelengths of 670.5 nm and 844.6 nm, which are sensitive to relatively hard and soft electrons, respectively. The fine spatial resolution of 9.5 deg field-of-view at magnetic zenith and the 100 Hz sampling rate of electron multiplying charge-coupled device (EMCCD) enabled us to resolve the spatiotemporal variation of the flickering aurora. It is found that there is only 10 ms time delay with 0.5 km spatial shift on average in the obtained flickering patterns at two wavelengths. The time delay and spatial shift can be comprehensively explained by the traveling inhomogeneous interference pattern of DAWs, probably associated with the Landau damping and/or time-of-flight effect, which is only detectable using the highest resolved temporal and spatial observations of flickering aurora. **Citation:** Kataoka, R., Y. Miyoshi, T. Sakanoi, A. Yaegashi, Y. Ebihara, and K. Shiokawa (2011), Ground-based multispectral high-speed imaging of flickering aurora, *Geophys. Res. Lett.*, *38*, L14106, doi:10.1029/2011GL048317.

1. Introduction

[2] Dispersive Alfven waves (DAWs) play an important role in an electromagnetic energy coupling process in the magnetosphere and ionosphere [*Chaston et al.*, 2008]. The ground-based imaging observations of terrestrial aurora can provide a unique opportunity to look into the DAW acceleration mechanisms. However, since the aurora generated by DAWs often contains spatial variations of less than 100 m and temporal variations faster than the video frame rate of 30 Hz, it had long been a challenging technical problem to image the aurora at sufficient resolution. *Semeter et al.* [2008] first reported a ground-based imaging observation of DAW-like aurora using a recently developed high-speed camera, utilizing an electron multiplying charge-coupled device (EMCCD).

[3] It has been suggested that DAWs are capable of accelerating electrons via Landau resonance to create flickering aurora [*Temerin et al.*, 1986]. *Sakanoi et al.* [2005] extended the idea of *Temerin et al.* [1986] and suggested that interference of multiple DAWs is essential to create typical morphological patterns of flickering aurora. *Gustavsson et al.* [2008] and *Whiter et al.* [2008] have showed that spatiotemporal variations of flickering aurora are consistent with the DAW interference theory. Recently, *Yaegashi et al.* [2011] showed consistent results supporting the DAW interference theory for flickering aurora with typical frequency below 15 Hz, and they found a new type of flickering aurora with high frequency of more than 20 Hz. *Whiter et al.* [2010] found that the flickering frequency is anti-correlated with the characteristic energy of precipitating electrons as expected from the DAW interference theory. Using multiple EMCCD cameras with different wavelengths, it may also be possible to detect the time difference of visible patterns at two different wavelengths, which can contribute to understanding the origin of the flickering aurora. The purpose of this paper is to show such a new capability of high-speed multispectral imaging observations.

2. Instrumentation

[4] We installed two EMCCD cameras during the winter season from January to April 2010 at Poker Flat Research Range where the geographic latitude and longitude are 65.1N and 147.4W, respectively. The magnetic latitude is 65.5 deg, and the magnetic midnight is about 1130 UT. Based on the photometer observations of *Ono et al.* [1992], we selected two different wavelengths of 670.5 nm and 844.6 nm to investigate the characteristic energy of precipitating electrons. The intensity ratio between 670.5 nm and 844.6 nm is known to be high for hard electrons and low for soft electrons [*Ono and Morishima*, 1994]. A Hamamatsu EMCCD camera equipped with a 50 mm/F0.95 lens with an 844.6-nm filter (center wavelength: 845.5 nm, band width (FWHM): 2.3 nm) was installed to measure relatively soft electrons through the auroral emissions from atomic oxygen [see also *Kataoka et al.*, 2011]. It was operated at a 110-Hz sampling rate by a 4×4 binning mode (128×128 pixels). An Andor Ixon EMCCD camera equipped with a 50 mm/F1.2 lens and a 670.5-nm filter (center wavelength: 670 nm, band width: 40 nm) was also installed to measure relatively hard electrons through the auroral emission from molecular nitrogen [see also *Yaegashi et al.*, 2011]. It was operated at a 100-Hz sampling rate by a 8×8 binning mode (64×64 pixels). The quantitative estimate of the average energy is beyond the scope of this paper, and we use the ratio itself as an indicator of characteristic energy to discuss the morphological pattern.

---

[1]Interactive Research Center of Science, Tokyo Institute of Technology, Tokyo, Japan.
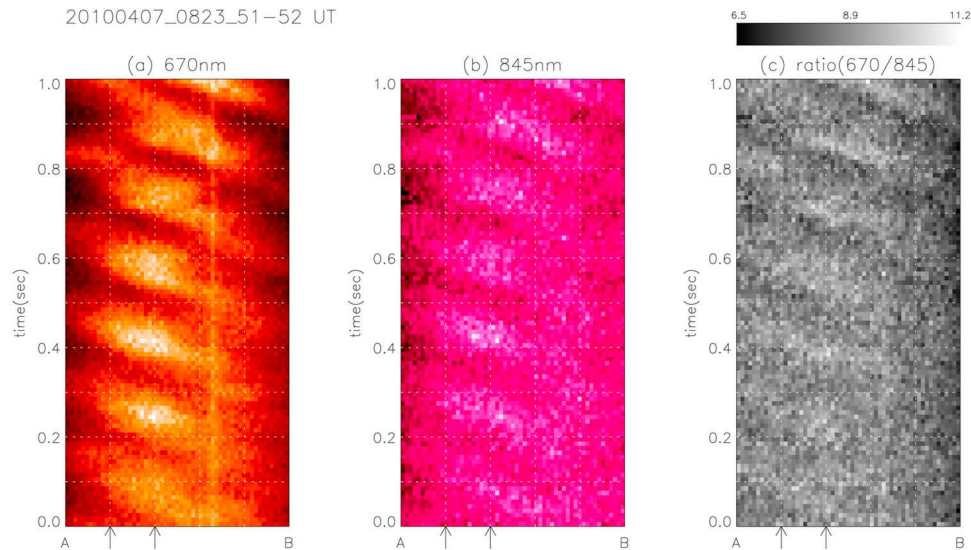[2]Solar-Terrestrial Environment Laboratory, Nagoya University, Nagoya, Japan.
[3]Planetary Plasma and Atmospheric Research Center, Tohoku University, Sendai, Japan.
[4]Research Institute for Sustainable Humanosphere, Kyoto University, Uji, Japan.

20100407_0823_51−52 UT

Figure 1. The time variation of flickering patches during one sec time interval from 08:23:51 UT to 08:23:52 UT on 7 April 2010. Time advances to the top, and magnetic east is to the left. The intensity is scaled in arbitrary unit and color coded at (a) 670 nm and (b) 845 nm with (c) the intensity ratio between Figures 1a and 1b, where the lighter color indicate larger value. The horizontal range from A to B corresponds to those in Animation 1, ranging about 14.3 km at 100 km altitude from East to West.

The typical energy of precipitating electrons associated with the flickering aurora has been known to range from a few keV to a few 10 keV [e.g., *Whiter et al.*, 2010].

[5] Artificial flashes of a light emitting diode synchronized with GPS-signals were observed every one minute by the two cameras at the same time to match the sampling time with an error less than 10 ms. The 110 Hz data is downsampled to be 100 Hz by the linear interpolation in time. Positions of a number of stars are used to match each pixel of two different images obtained by the two cameras. The fields of view of two cameras are 9.5 deg × 9.5 deg, which is about 16 km × 16 km at 100 km altitude, centered at magnetic zenith. After applying all of the calibrations and spatiotemporal matching of two cameras, final images used in this study consist of 58 × 58 pixels (FOV = 8.5 × 8.5 deg) at a sampling rate of 100 Hz.

3. Results and Discussions

[6] Animation 1 shows an example of dynamic evolution of flickering aurora for one sec time interval.[1] The flickering aurora was observed during a recovery phase of an auroral breakup which occurred during the recovery phase of a magnetic storm on 7 April 2010. The flickering aurora event occurred at 0823 UT in the pre-midnight sector (20.9 magnetic local time). The location of magnetic zenith is the very central pixel of the images.

[7] Figure 1 shows the time variation of flickering patches at 670.5 nm (Figure 1a) and 844.6 nm (Figure 1b). The horizontal range from A to B corresponds to 14.3 km at 100 km altitude, from East to West. To obtain higher signal to noise ratio, the intensity is vertically averaged within the white box in Animation 1 at each step. The flickering patches move eastward at approximately 50–60 km/s, and the frequency is about 6 Hz, as clearly seen in Figure 1a. From the intensity ratio between at the two wavelengths (Figure 1c), it is found

that the leading edge of each flickering patch, i.e. eastward side of patch, tends to be more energetic than the trailing part, as identified by the subtle change in brightness of a cut through Figure 1c taken at a constant time, most clearly exemplified for t > 0.6 s. From a standard lag-correlation analysis between Figures 1a and 1b, it is found that the images at 845 nm have a systematic time delay of 10 ms (1 frame), and a systematic spatial shift of 0.5 km (2 pixels) in the West direction, relative to the 670 nm signal.

[8] Since the intensity ratio should be the ratio of integrated volume emission rate along the magnetic field line, the energy dependence of the ratio is only strictly valid for observations directly in the magnetic zenith. In our imaging observations, the emissions come from very different altitude ranges, and the difference in altitude between the emitting layers is sensitive to the energy of the primary electrons [e.g., *Zettergren et al.*, 2007, Figure 5]. The emission ratio in this study is therefore sensitive to aspect angle to the magnetic field line, even over this small field of view.

[9] First, let us estimate some essential parameters assuming a simple beat pattern of two DAWs with two different angular frequencies $\omega - \alpha$ and $\omega + \alpha$. From a simple formula of trigonometric function, $\sin(\omega - \alpha)t + \sin(\omega + \alpha)t = 2\sin\omega t \cos\alpha t$. Also assuming the two different wave numbers of $k - \beta$ and $k + \beta$ perpendicular to the ambient magnetic field, the phase speed ω/k of a flickering pattern at angular frequency ω provides the mean perpendicular wave number k. From Figure 1, the phase speed at 100 km altitude is about 50–60 km/s and the frequency is about 6 Hz, the perpendicular wavelength of the DAWs mapped onto the 100 km altitude is therefore 8–10 km as calculated from the observed phase speed and the frequency. There is another way to estimate the perpendicular wavelength of DAWs, assuming that the patch size is a half of the perpendicular wavelength mapped onto the ionosphere. The apparent patch size is 3–5 km, and the perpendicular wavelength will be 6–10 km. The perpendicular wave number of a DAW calculated from

---

[1]Animations are available in the HTML.
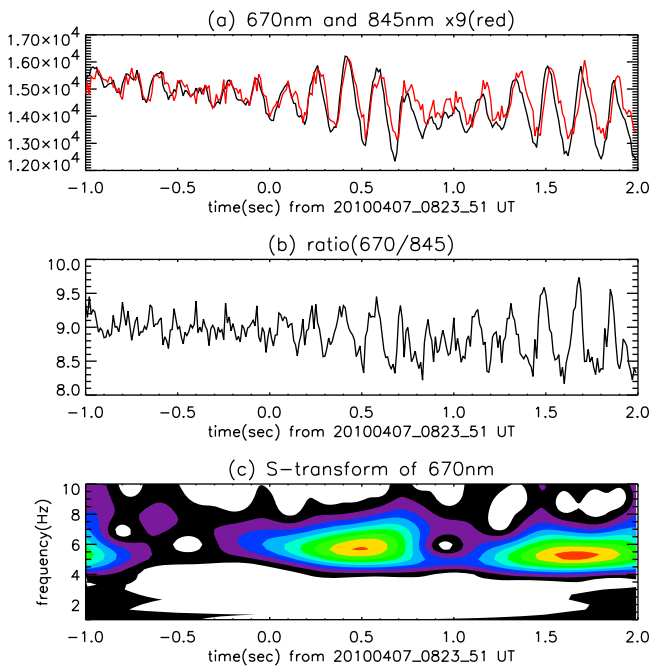
Figure 2. The intensity profiles at (a) 670 nm and 845 nm in arbitrary unit with (b) the ratio, spatially averaged Figures 1a–1c over the region from one fifth to the two fifth between the points A and B. (c) The S-transform spectrum of the 670 nm intensity profile.

the flickering patch speed and frequency matches the perpendicular wave number of a DAW calculated from the patch size, and so the observations fit well with the DAW interference theory for flickering aurora generation.

[10] Second, we estimate the time delay as a result of a simple time-of-flight (TOF) effect. The small time delay suggests that either the source of the precipitating electrons is low in altitude or the energy distribution is narrow. If we assume the Landau resonance of 6 Hz O+ electromagnetic ion cyclotron waves with electrons at the maximum phase velocity, the resonance altitude and energy are about 3000 km and 4.1 keV, respectively, under the low plasma density condition of ~10/cc above 3000 km [see *Whiter et al.*, 2010, Figure 5]. The energy distribution of flickering electrons is, for example, as narrow as ranging from 3.3 keV to 4.1 keV to explain the 10 ms TOF dispersion.

[11] Third, we show that both the time delay and spatial shift can be comprehensively explained by traveling inhomogeneous patchy patterns. The traveling speed, i.e. the perpendicular phase velocity, is about 50–60 km/s in the east-west direction at the ionosphere as estimated in the previous section. The patches, as manifested in the two wavelengths, are offset from one another by 0.5 km in the horizontal. The 10 ms time delay is in fact comparable with the time delay expected from the 0.5 km shifted patches with the traveling speed of 50–60 km/s. In the resonant altitude, considering a simple dipole magnetic field, the traveling speed is scaled as about 100 km/s and the spatial difference at the leading edge is scaled as about 1 km. The traveling speed is more than two orders of magnitude smaller than the local Alfven speed of a few tens of thousand km/s at a typical resonant altitude of

several thousand km, which is consistent with the existence of acceleration associated with obliquely propagating Alfven waves, i.e. DAWs.

[12] The same lag-correlation analysis was applied for the time intervals 1 s before and after the event. It is found that the time delay and spatial shift are 10 ms (20 ms) and 0.74 km (0.74 km) for 1 s before (after) the event, respectively. Figure 2a shows the intensity profiles for the 3 s time interval at 670 nm and 845 nm. The intensities are calculated by spatially (horizontally) averaging Figures 1a and 1b over the region from one fifth to the two fifth between the points A and B as shown by arrows, where the flickering patches are best captured. The averaged time delay is getting larger as shown in the difference of 670 nm and 845 nm in Figure 2a. As shown in the S-transform [*Stockwell et al.*, 1996] of the 670 nm profile (Figure 2c), the typical frequency decreases from 6 Hz to 5 Hz for the 3 s time interval, although the first 1 s is relatively obscure. The ratio in Figure 2b, indicator of characteristic energy of precipitating electrons, tends to have high peak values for the last 1 s time interval when the frequency is small, which is consistent with the finding of *Whiter et al.* [2010]. The elongated time delay is consistent with the enhanced maximum energy of Landau resonance, for if the highest energies are increasing, and the low energy contribution is unchanged, the time delay of TOF would be increased. Note also that the increasing delay between 670 nm and 845 nm as shown in Figure 2a is not consistent with the perspective effect simply because the overall position of traveling patches does not change.

[13] From Figures 2a and 2b, we confirm that the leading front part is more energetic than the trailing part. As illustrated by *Semeter et al.* [2008], more energetic leading front than the trailing part may indicate that DAWs lose energy associated with the Landau damping, although detailed examination of such a DAW acceleration process associated with the interference potential pattern remains as an important future work. Also, this paper cannot discriminate between the TOF effect and the Landau damping pattern as the TOF effect appears in the same sense to enhance the Landau damping pattern. So far this is the only beautiful flickering event in which we can compare the images at two different wavelengths in detail, and more thorough statistical study using the whole database is ongoing. A possible beat pattern of 1 Hz as appeared in Figure 2a may be an interesting future topic to be investigated to further test the interference model.

References

Chaston, C. C., C. Salem, J. W. Bonnell, C. W. Carlson, R. E. Ergun, R. J. Strangeway, and J. P. McFadden (2008), The turbulent Alfvenic aurora, *Phys. Rev. Lett.*, *100*(17), 175003, doi:10.1103/PhysRevLett.100. 175003.

Gustavsson, B., J. Lunde, and E. M. Blixt (2008), Optical observations of flickering aurora and its spatiotemporal characteristics, *J. Geophys. Res.*, *113*, A12317, doi:10.1029/2008JA013515.

Kataoka, R., Y. Miyoshi, T. Sakanoi, A. Yaegashi, K. Shiokawa, and Y. Ebihara (2011), Turbulent microstructures and formation of folds in auroral breakup arc, *J. Geophys. Res.*, *116*, A00K02, doi:10.1029/2010JA016334.

Ono, T., and K. Morishima (1994), Energy parameters of precipitating auroral electrons obtained by using photometric observations, *Geophys. Res. Lett.*, *21*(4), 261–264, doi:10.1029/94GL00011.

Ono, T., R. Satake, T. Yoshino, and T. Hirasawa (1992), Energy parameters of the incident auroral electrons derived by the intensity ratio of auroral emissions, *Antarct. Rec.*, *36*(2), 163–180.

Sakanoi, K., H. Fukunishi, and Y. Kasahara (2005), A possible generation mechanism of temporal and spatial structures of flickering aurora, *J. Geophys. Res.*, *110*, A03206, doi:10.1029/2004JA010549.

Semeter, J., M. Zettergren, M. Diaz, and S. Mende (2008), Wave dispersion and the discrete aurora: New constraints derived from high-speed imagery, *J. Geophys. Res.*, *113*, A12208, doi:10.1029/2008JA013122.

Stockwell, R. G., L. Mansinha, and R. P. Lowe (1996), Localization of the complex spectrum: The S transform, *IEEE Trans. Signal Processing*, *44*(4), 998–1001, doi:10.1109/78.492555.

Temerin, M., J. McFadden, M. Boehm, C. Carlson, and W. Lotko (1986), Production of flickering aurora and field-aligned electron flux by electromagnetic ion cyclotron waves, *J. Geophys. Res.*, *91*(A5), 5769–5792, doi:10.1029/JA091iA05p05769.

Whiter, D. K., B. S. Lanchester, B. Gustavsson, N. Ivchenko, J. M. Sullivan, and H. Dahlgren (2008), Small-scale structures in flickering aurora, *Geophys. Res. Lett.*, *35*, L23103, doi:10.1029/2008GL036134.

Whiter, D. K., B. S. Lanchester, B. Gustavsson, N. Ivchenko, and H. Dahlgren (2010), Using multispectral optical observations to identify the acceleration mechanism responsible for flickering aurora, *J. Geophys. Res.*, *115*, A12315, doi:10.1029/2010JA015805.

Yaegashi, A., T. Sakanoi, R. Kataoka, K. Asamura, Y. Miyoshi, M. Sato, and S. Okano (2011), Spatial-temporal characteristics of flickering aurora as seen by high-speed EMCCD imaging observations, *J. Geophys. Res.*, *116*, A00K04, doi:10.1029/2010JA016333.

Zettergren, M., J. Semeter, P.-L. Blelly, and M. Diaz (2007), Optical estimation of auroral ion upflow: Theory, *J. Geophys. Res.*, *112*, A12310, doi:10.1029/2007JA012691.

Y. Ebihara, Research Institute for Sustainable Humanosphere, Kyoto University, Uji 611-0011, Japan.

R. Kataoka, Interactive Research Center of Science, Tokyo Institute of Technology, Tokyo 152-8551, Japan. (ryuho@geo.titech.ac.jp)

Y. Miyoshi and K. Shiokawa, Solar-Terrestrial Environment Laboratory, Nagoya University, Nagoya 464-8601, Japan.

T. Sakanoi and A. Yaegashi, Planetary Plasma and Atmospheric Research Center, Tohoku University, Sendai 980-8578, Japan.